8-2011

Ultrathin BaTiO3 templates for multiferroic nanostructures

Xumen Chen
University of Nebraska-Lincoln

Seolun Yang
Sook-Myung Women's University, Seoul, Korea

Ji-Hyun Kim
Sook-Myung Women's University, Seoul, Korea

Hyung-Do Kim
Pohang Acceleration Laboratory (PAL), Pohang, Korea

Jae-Sung Kim
Sook-Myung Women's University, Seoul, Korea

See next page for additional authors

Authors
Xumen Chen, Seolun Yang, Ji-Hyun Kim, Hyung-Do Kim, Jae-Sung Kim, Geoffrey Rojas, Ralph Skomski, Haidong Lu, Anand Bhattacharya, Tiffany Santos, Nathan Guisinger, Matthias Bode, Alexei Gruverman, and Axel Enders

New Journal of Physics
The open-access journal for physics

Ultrathin $BaTiO_3$ templates for multiferroic nanostructures

Xumin Chen[1], Seolun Yang[2], Ji-Hyun Kim[2], Hyung-Do Kim[3], Jae-Sung Kim[2], Geoffrey Rojas[1], Ralph Skomski[1,4], Haidong Lu[1], Anand Bhattacharya[5], Tiffany Santos[5], Nathan Guisinger[5], Matthias Bode[5], Alexei Gruverman[1] and Axel Enders[1,4,6]

[1] Department of Physics and Astronomy, University of Nebraska-Lincoln, Lincoln, NE 68588, USA
[2] Department of Physics, Sook-Myung Women's University, Seoul 140-742, Korea
[3] Beamline Division, Pohang Acceleration Laboratory (PAL), Pohang 790-784, Korea
[4] Nebraska Center for Materials and Nanoscience (NCMN), University of Nebraska, Lincoln, NE, USA
[5] Center for Nanoscale Materials, Argonne National Laboratory, Argonne, IL 60439, USA
E-mail: a.enders@me.com

New Journal of Physics **13** (2011) 083037 (10pp)
Received 16 March 2011
Published 31 August 2011
Online at http://www.njp.org/
doi:10.1088/1367-2630/13/8/083037

Abstract. The structural, electronic and dielectric properties of high-quality ultrathin $BaTiO_3$ films were investigated. The films, which were grown by ozone-assisted molecular beam epitaxy on Nb-doped $SrTiO_3(001)$ substrates and have thicknesses as low as 8 unit cells (u.c.) (3.2 nm), are unreconstructed and atomically smooth with large crystalline terraces. A strain-driven transition to three-dimensional (3D) island formation is observed for films of 13 u.c. thickness (5.2 nm). The high structural quality of the surfaces, together with dielectric properties similar to bulk $BaTiO_3$ and dominantly TiO_2 surface termination, makes these films suitable templates for the synthesis of high-quality metal-oxide multiferroic heterostructures for the fundamental study and exploitation of magneto-electric effects, such as a recently proposed interface effect in $Fe/BaTiO_3$ heterostructures based on Fe–Ti interface bonds.

S Online supplementary data available from stacks.iop.org/NJP/13/083037/mmedia

[6] Author to whom any correspondence should be addressed.

Contents

1. Introduction

The coexistence of ferroelectricity and ferromagnetism in two-phase multiferroic systems comprising metals and oxides can result in interesting and useful phenomena, such as magneto-electric effects [1]. One model two-phase system exhibiting magneto-electric behavior, that is, electric field dependence of magnetization, is epitaxial Fe on $BaTiO_3$ substrates. The magnetic anisotropy of Fe, observable as the magnitude of the coercive field, depends strongly on $BaTiO_3$'s electric polarization, as has been shown by Sahoo *et al* [2]. The underlying mechanism here is a lateral strain exerted by the ferroelectric on the ferromagnet and the associated change in the magneto-elastic contribution to the total magnetic anisotropy. A second mechanism, different in nature but also leading to magneto-electric behavior, has been predicted recently for $Fe/BaTiO_3$ heterostructures [3, 4]. Characteristic of this new effect are modulations of the Fe–Ti bonds at the interface by the piezo-electric distortion of the $BaTiO_3$, resulting in changes in the effective magnetic moments of Fe and Ti atoms and the anisotropy. A second and related example is magnetic tunnel junctions, which are also based on metal-oxide interfaces [5]. Experimental investigation of any metal-oxide heterostructures depends critically on the quality of the oxide layer, since their performance is extremely sensitive to the chemical and structural properties of the interfaces. The realization of model structures or even devices exhibiting and exploiting the above effects is complicated by the experimental difficulty of growing metal-oxide interfaces of sufficiently high interface quality.

Atomically smooth $BaTiO_3$ substrates are a requirement for the study of magneto-electric effects in all $BaTiO_3$-based heterostructures. They can be obtained by annealing bulk samples under ultrahigh vacuum or in hydrogen atmosphere to temperatures around 1000 K [6–8], but both the atomic structure and the surface termination depend critically on the preparation conditions [8–10]. As an alternative to bulk $BaTiO_3$ substrates, ultrathin films of $BaTiO_3$ were prepared and studied recently [11–27]. Their structural characterization has so far been limited to reflection high-energy electron diffraction (RHEED) during growth [17, 19, 20, 25, 28], and low-energy electron diffraction (LEED) [12]. It is known from these studies that the films grow layer by layer only below a critical film thickness, which is of the order of 12 unit cells (u.c.) [18]. Characterization by piezo-response force microscopy (PFM) [29] has demonstrated robust ferroelectricity in films with thickness as low as 1 nm (under compressive strain) [30], and layers with thickness as low as 1 u.c. can be ferroelectric in $BaTiO_3/SrTiO_3$ superlattices (1 u.c. = 0.399 nm). However, a comprehensive *in situ* characterization with surface-sensitive methods to address the atomistic structure, surface termination and dielectric properties is currently lacking, but is urgently required for the optimization of synthesis strategies and to achieve a significant performance increase in magneto-electric structures.

This paper aims to fill this gap. We present a comprehensive study of the structural, dielectric and electronic properties of $BaTiO_3$ films, which are only a few u.c. thick and grown on Nb-doped $SrTiO_3$ substrates, with a combination of local probe methods and electron diffraction and spectroscopy. We will demonstrate that such films are superior to bulk $BaTiO_3$ substrates regarding the structural quality at the surface, while still showing the dielectric properties of bulk $BaTiO_3$. We propose that $BaTiO_3$ thin films are suitable for fundamental research and applications, such as for the study of magneto-electric effects and magneto-tunnel junctions.

2. Experimental procedure

The $BaTiO_3$ films were grown by molecular beam epitaxy (MBE) by co-evaporation of Ba and Ti from Knudsen cells and using pure ozone as the oxidizing agent. A steady flow of ozone gas was delivered to the growth chamber with the pressure maintained at 2×10^{-6} torr. Prior to film growth, the Nb : $SrTiO_3$ substrates (0.2% Nb doping) were prepared with a buffered HF dip to obtain a TiO_2-terminated surface. The substrate was heated in ozone to a growth temperature of 650 °C and then cooled in ozone after film deposition. Each $BaTiO_3$ unit cell was deposited in ∼50 s followed by 30 s annealing (with Ba and Ti shutters closed). The deposition was monitored using RHEED.

After growth, the samples were transferred through air into separate ultrahigh vacuum systems for further studies with scanning tunneling microscopy (STM), LEED, photoemission spectroscopy (UPS), etc. While immediately after transfer no LEED pattern was observable, extremely sharp (1×1) diffraction patterns could be established by thermal annealing at approximately 650 K under O_2 pressure of 3.75×10^{-7} torr, using an oxygen doser that faces the sample surface at a distance of ∼5 cm. STM images were taken at 45 K using an Omicron variable temperature STM. Photoelectron spectroscopy (PES) was carried out at a soft x-ray beam line (3A1) at the Pohang Light Source, Korea. The UPS spectra presented here were taken with the sample kept at room temperature using a hemispherical electron energy analyzer with multichannel detector (Scienta). The energy resolution is 0.3 eV, as determined from the measured shape of Fermi edge of a Cu reference sample. The binding energy is measured with respect to the Fermi edge of Cu. PFM measurements were carried out in air [31, 32, 39]. An external ac bias voltage is applied to the PFM tip, and the local piezo-electric response from the ferroelectric layer was measured. By scanning the sample surface a two-dimensional (2D) map of the piezo-response amplitude and phase signals could be generated, providing information on the polarization magnitude and direction. For local hysteresis loop measurement, a dc offset voltage of controlled magnitude is applied to the tip. Dielectric properties, such as the coercive field and remanent polarization, were deduced from local hysteresis loops.

3. Results and discussion

3.1. Surface morphology studies with scanning tunneling microscopy

Our studies focus on $BaTiO_3$ films of 8 and 13 u.c. thickness. RHEED images taken along the [100] axis of the pristine Nb : $SrTiO_3$ substrate surface prior to film growth and of the

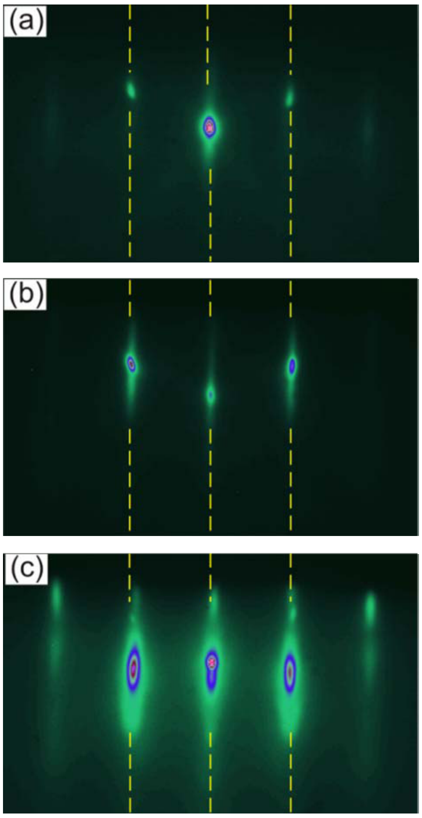

Figure 1. RHEED images of $BaTiO_3$ grown by MBE, taken at different stages of growth. (a) Pristine Nb-$SrTiO_3$(100) substrate; (b) after growth of 8 u.c. of $BaTiO_3$; and (c) after growth of 13 u.c. of $BaTiO_3$.

8 and 13 u.c. $BaTiO_3$ films are shown in figures 1(a)–(c), respectively. In particular, for the 8 u.c. film, spots rather than streaks were observed (figure 1(b)), which is consistent with large, crystalline terraces at the surface of the films. Those spots broaden into streaks as the film thickness is increased to 13 u.c., indicating a gradual increase in the surface roughness (figure 1(c)). The films were transferred through air into a separate STM UHV chamber after growth, where they were annealed in oxygen to recover ordered LEED diffraction patterns. A weak LEED pattern became observable at an annealing temperature of $T_a = 150\,°C$. With increasing temperature the peak intensity and sharpness improved and the background intensity decreased until high-quality (1×1) diffraction patterns were observed at $T_a \sim 650–700\,°C$ (figure 2). Further annealing was found to be detrimental to the diffraction image quality. STM images were taken on both films immediately after the annealing, at a sample temperature of 45 K. Flat terraces of approximately 100 nm width were found on the 8 u.c. film and the terrace step height corresponds to a single unit cell of $BaTiO_3$ (figure 2). Despite the atomically smooth terraces, the films are not expected to be globally smooth because of the potential existence of twin boundaries, even though they were not observed in this study. The 13 u.c. films also exhibit atomically flat terraces; however, the terraces are now covered with small islands of average diameter ~10 nm. A height histogram analysis reveals that there are on average four open layers (not shown here). This is also consistent with the observation of streaks in the RHEED images and is attributed to the relaxation of epitaxial film strain. It is concluded that crystalline films

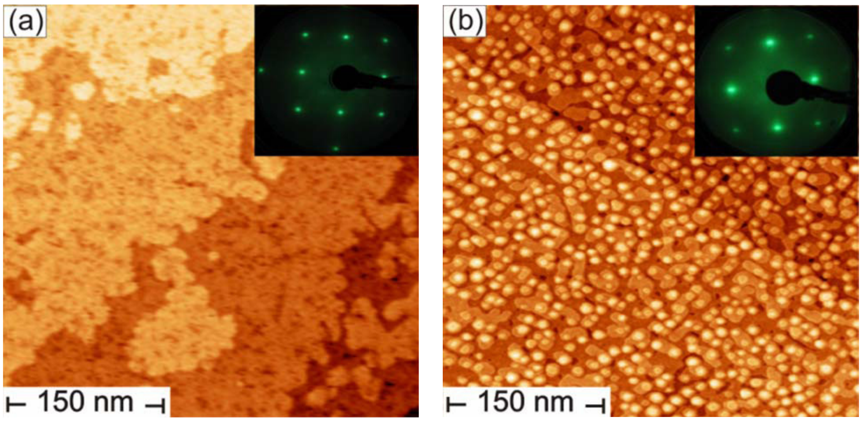

Figure 2. STM images and LEED patterns of $BaTiO_3$ films on Nb-$SrTiO_3$. The thickness of $BaTiO_3$ films is 8 u.c. (a) and 13 u.c. (b). The LEED images were taken at 85 eV.

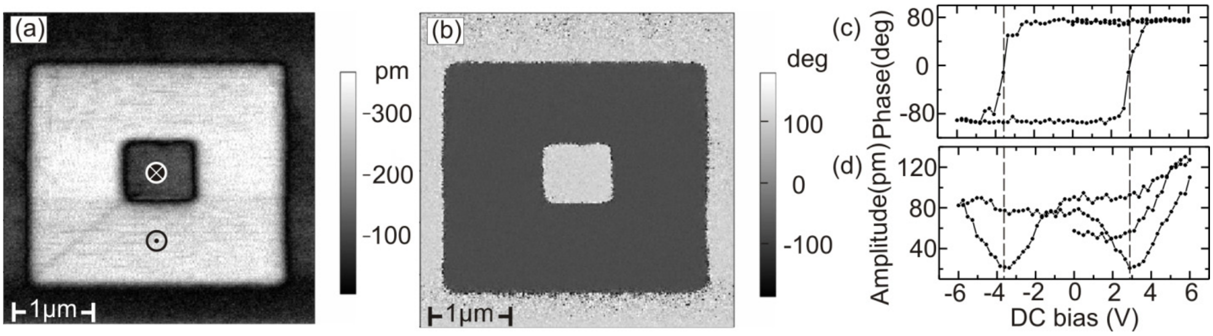

Figure 3. Maps of the remanent PFM amplitude signal (a) and phase signal (b) of a $BaTiO_3$(8 u.c.)/Nb-$SrTiO_3$ film, showing areas of opposite ferroelectric polarization, produced by scanning with the tip under ±4 V dc bias. Hysteresis loops of the PFM in-field phase (c) and amplitude (d) acquired from the same film.

showing no detectable surface reconstruction and exhibiting terraces as wide as 100 nm in the case of the 8 u.c. film can be recovered after sample transfer through air.

3.2. Piezo-response force microscopy and dielectric properties

Resonance-enhanced PFM measurements [31, 32] have been carried out at room temperature on the $BaTiO_3$ films in air after extraction of the samples from the growth chamber, without further sample treatment. Prior to PFM characterization, bi-domain square-in-square polarization patterns have been generated in the $BaTiO_3$ films by scanning the surface with an applied dc bias voltage of ±4 V. The PFM phase and amplitude maps of the resulting patterns, together with local polarization hysteresis loops, are shown in figure 3 for 8 u.c.-thick films. Identical results were obtained from 13 u.c.-thick films and are not shown here, for brevity. The amplitude signal in figure 3(a) is a measure of the polarization magnitude, whereas the phase signal in figure 3(b) shows the polarization direction. The hysteresis loops of the phase and the amplitude signals in panels (c) and (d) confirm the existence of non-zero remanent polarization, which can be

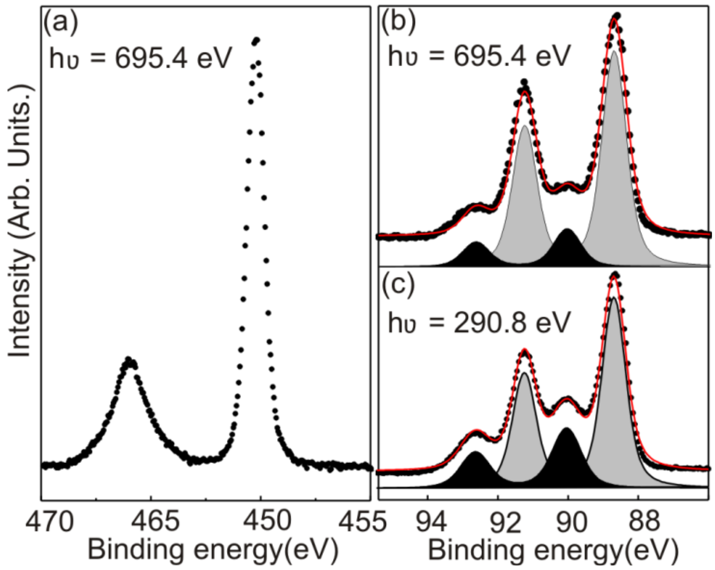

Figure 4. Photoelectron spectra of $BaTiO_3(001)$. Ti 2p spectrum (a) and Ba 4d spectra taken at 695.4 eV (b) and 290.8 eV (c), respectively, are shown. The binding energy is in reference to Fermi energy. Black- and gray-shaded areas in (b, c) represent fits to the bulk and surface peaks of Ba $4d_{5/2}$ and $4d_{3/2}$, respectively.

reversed by applying electric fields larger than those corresponding to the measured coercive bias voltage of approximately 3.5 V. The visible asymmetry in the amplitude signal hysteresis loop for opposite polarization is due to differences in the interfaces on both sides of the $BaTiO_3$. Film boundaries and surface terminations are known to result in the accumulation of surface charges, which influence the symmetry of the observed PFM loops.

3.3. Photoelectron spectroscopy and surface termination

PES data have been collected on the 13 u.c. $BaTiO_3$ film, to determine the surface termination and to learn about the electronic structure of such films. Even though the growth of the films was stopped after deposition of the TiO_2 layer, the actual surface termination after transfer through air and annealing in oxygen needs verification. The Ba 4d and the Ti 2p spectra are summarized in figure 4. The Ti 2p spectrum shows two characteristic peaks identified as the Ti $2p_{3/2}$ and Ti $2p_{1/2}$ peaks. In these spectra, no surface core level shift (SCLS) is observable. Such a shift is often observed at surfaces due to the reduced coordination of the atoms and the resulting change in charge state there. However, to the best of our knowledge, no SCLS has ever been reported for TiO_2-terminated surfaces. The absence of SCLS for the Ti 2p peaks can be expected, because the effective charge of Ti ions in the TiO_2-terminated $BaTiO_3$ surface is similar to that of Ti ions in the bulk $BaTiO_3$, as has been predicted in first-principles calculations [10]. Thus, the absence of SCLS of Ti does not exclude TiO_2 surface termination.

By contrast, the effective charge of Ba ions in a BaO-terminated surface is less than half that of Ba ions in the bulk, thereby producing substantial SCLS, as has already been reported for bulk $BaTiO_3(001)$ [33]. For the present films, we found that the 4d peaks of Ba split into the well-known $4d_{5/2}$ and $4d_{3/2}$ peaks, and two additional peaks shifted by $\sim$1.5 eV towards higher binding energies with respect to those 4d peaks (figures 4(b) and (c)). Similarly,

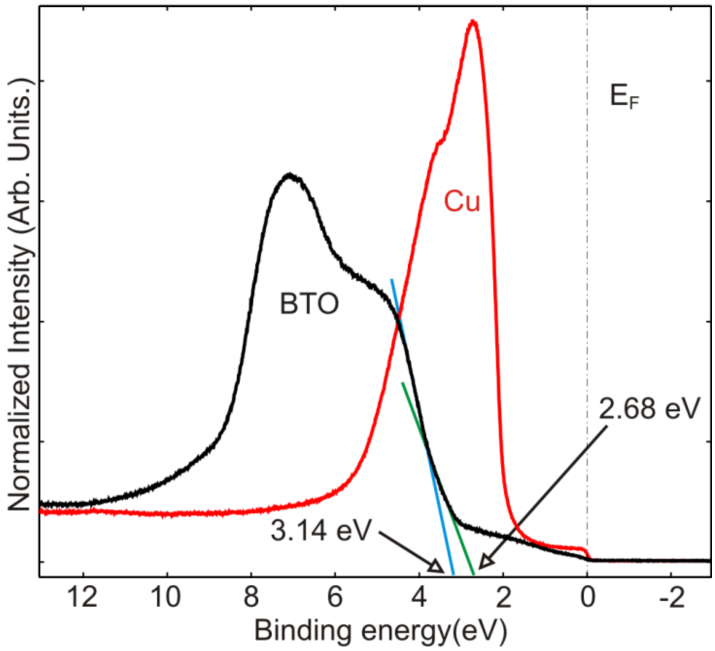

Figure 5. Photoelectron spectra near the Fermi edge of clean $BaTiO_3(001)$ and Cu. The photon energy was 111.04 eV. Extrapolating the band edges gives the band gap (blue and green lines). The non-zero signal in the band gap is due to the existence of mid-gap states (see text).

shifted peaks have been reported for BaO surface layers and are ascribed to SCLS [34]. Ba 4d spectra have been taken with two different photon energies, 695.4 and 290.8 eV. We observe an increase in the ratio of surface to bulk peaks at lower photon energies, where the photoelectrons have smaller kinetic energy and are thus more surface-sensitive. Both observations, the SCLS and the energy dependence of the surface to bulk peak ratio of the Ba 4d states, suggest the existence of BaO on the surface of the films; however, to perform a quantitative analysis of the fractions of BaO- and TiO_2-terminated surface areas requires a detailed analysis of the photoemission peak intensities.

The standard approach for the peak intensity analysis in PES [37] has been adapted here for surfaces containing two atomic species. A detailed discussion of the spectral areas of the Ba 4d bulk and SCLS peak pairs is given in the supplementary material (stacks.iop.org/NJP/13/083037/mmedia). We conclude from this analysis that the $BaTiO_3$ layer is dominantly TiO_2-terminated, specifically we find the fractions of the TiO_2- and BaO-terminated surface areas to be ∼70 and ∼30%, respectively. Uncertainties in our analysis result from estimates of the electron mean free path. We performed further complementary experiments with angular-dependent photoemission spectroscopy on several $BaTiO_3$ thin films on $SrTiO_3$ and $LaSrMO_3$ substrates, fabricated by different groups. Those samples have been prepared at varied annealing temperatures (200–650 °C) and oxygen partial pressures under UHV. All measurements consistently find surfaces dominantly terminated by TiO_2. We conclude that the TiO_2 termination of $BaTiO_3(001)$ films is energetically favored and robust during *in situ* sample preparation.

The valence band spectra of the $BaTiO_3$ samples are shown in figure 5, together with the spectra of a Cu reference sample for comparison. Most prominently, the valence band, which is mostly of O 2p character, spans from ∼3 to 10 eV binding energy. The width of the band gap is determined by extrapolating the band edge. This is shown in figure 5 for two extreme choices of linear extrapolations, resulting in upper and lower limits for the band gap of 2.7–3.2 eV, respectively. In-gap states are observable between the valence band edge and the Fermi edge. Such states are most commonly found to originate from oxygen defects [33, 35, 36] and Ti 3+ ions located in the vicinity of oxygen defects [36]. While first-principles calculations predict that the valence band reaches the Fermi edge [35], we observe instead a band shift to higher binding energy. This shift is similar to the optical band gap of $BaTiO_3$ of 3.22 eV. It is reasonable to attribute this shift to the pinning of the Fermi level at the bottom of the conduction band to the effective n-type doping, which is a result of the reduction of the sample during the annealing. This indicates that the film has a band gap analogous to bulk $BaTiO_3$, with in-gap states due to local defects. The latter finding is not surprising for the 13 u.c. film given the observed transition to a 3D island structure.

4. Conclusions

The nanometer-thick films of $BaTiO_3$ studied in this paper have the following advantages over bulk samples: the formation of large, atomically smooth surface terraces of 1 u.c. height and the absence of surface reconstruction, while still being insulating and exhibiting remanent electric polarization. Our samples show distinctively improved dielectric properties compared with the epitaxial BTO films published so far. Ultrathin $BaTiO_3$ films are thus expected to become substrates for the fabrication of various model systems for the study of magneto-electric effects and also to facilitate theoretical analysis. An important result of this paper is the demonstration that high-quality surfaces of $BaTiO_3$ can be recovered after sample transfer through air. This will simplify the sample exchange in most laboratory settings where oxide growth, surface analytics and device fabrication are done in separate UHV systems. We have shown that BaO and TiO_2 surface terminations can coexist and are thus similar in energy, thereby providing experimental evidence to support the mostly theory-based discussion in the literature. Due to the prevalent TiO_2 termination of the surface, these films potentially enable one to synthesize high-quality $Fe/BaTiO_3$ interfaces that might exhibit the recently proposed magneto-electric effect due to Fe–Ti-bond modulation.

Acknowledgments

This work was supported by the NSF through CAREER (DMR-0747704) and MRSEC (DMR-0213808), by the US Department of Energy (DE-SC0004876) and by the NRF (2007-0055035). The use of the facilities at the Center for Nanoscale Materials was supported by the US Department of Energy, Office of Science, Office of Basic Energy Sciences, under contract no. DE-AC02-06CH11357.

References

[1] Ramesh R and Spaldin N A 2007 Multiferroics: progress and prospects in thin films *Nat. Mater.* **6** 21

[2] Sahoo S, Polisetty S, Duan C-G, Jaswal S S, Tsymbal E Y and Binek C 2007 Ferroelectric control of magnetism in $BaTiO_3/Fe$ heterostructures via interface strain coupling *Phys. Rev.* B **76** 092108

[3] Duan C-G, Jaswal S S and Tsymbal E Y 2006 Predicted magnetoelectric effect in Fe/$BaTiO_3$ multilayers: ferroelectric control of magnetism *Phys. Rev. Lett.* **97** 047201
[4] Duan C-G, Velev J P, Sabirianov R F, Mei W-N, Jaswal S S and Tsymbal E Y 2008 Tailoring magnetic anisotropy at the ferromagnetic/ferroelectric interface *Appl. Phys. Lett.* **92** 122905
[5] Dimopoulos T, Da Costa V, Tiusan C, Ounadjela K and van den Berg H A M 2001 Interfacial phenomena related to the fabrication of thin Al oxide tunnel barriers and their thermal evolution *Appl. Phys. Lett.* **79** 3110
[6] Shimitzu T, Bando H, Aiura Y, Haruyama Y, Oka K and Nishimura Y 1995 Scanning tunneling microscopy and spectroscopy observation of reduced $BaTiO_3$(100) surface *Japan. J. Appl. Phys.* **34** L1305
[7] Bando H, Shimitzu T, Aiura Y, Haruyama Y, Oka K and Nishimura Y 1996 Structure and electronic states on reduced $BaTiO_3$ surface observed by scanning tunneling microscopy and spectroscopy *J. Vac. Sci. Technol.* B **14** 1060
[8] Kolpak A M, Li D, Shao R, Rappe A M and Bonnel D A 2008 Evolution of the structure and thermodynamic stability of the $BaTiO_3$(001) surface *Phys. Rev. Lett.* **101** 036102
[9] Rakotovelo G, Moussounda P S, Haroun M F, Legaré P, Rakotomahevitra A and Parlebas J C 2007 DFT study of $BaTiO_3$(001) surface with O and O_2 adsorption *Eur. Phys. J.* B **57** 291
[10] Xue X Y, Wang C L and Zhong W L 2004 The atomic and electronic structure of the TiO_2- and BaO-terminated $BaTiO_3$(001) surfaces in a paraelectric phase *Surf. Sci.* **550** 73
[11] Wills L A, Wessels B W, Richeson D S and Marks T J 1992 Epitaxial growth of $BaTiO_3$ thin films by organometallic chemical vapor deposition *Appl. Phys. Lett.* **60** 41
[12] Shin J, Nascimento V B, Borisevich A Y, Plummer E W, Kalinin S V and Baddorf A P 2008 Polar distortion in ultrathin $BaTiO_3$ films studied by in situ LEED I–V *Phys. Rev.* B **77** 245437
[13] Shin J, Kalinin S V, Plummer E W and Baddort A P 2009 Electronic transport through in situ grown ultrathin $BaTiO_3$ films *Appl. Phys. Lett.* **95** 032903
[14] Sun H, Tian W, Pan X, Haeni J H and Schlom D G 2004 Evolution of dislocation arrays in epitaxial $BaTiO_3$ thin films grown on (100) $SrTiO_3$ *Appl. Phys. Lett.* **84** 3298
[15] Tenne D A *et al* 2006 Probing nanoscale ferroelectricity by ultraviolet Raman spectroscopy *Science* **313** 1614
[16] Tenne D A *et al* 2009 Ferroelectricity in ultrathin $BaTiO_3$ films: probing the size effect by ultraviolet Raman spectroscopy *Phys. Rev. Lett.* **103** 177601
[17] Shigetani H, Kobayashi K, Fujimoto M, Sugimura W, Matsui Y and Tanaka J 1997 $BaTiO_3$ thin films grown on $SrTiO_3$ substrates by a molecular-beam-epitaxy method using oxygen radicals *J. Appl. Phys.* **81** 693
[18] Visinoiu A, Alexe M, Lee H N, Zakharov D N, Pignolet A, Hesse D and Goesele U 2002 Initial growth stages of epitaxial $BaTiO_3$ films on vicinal $SrTiO_3$(001) substrate surfaces *J. Appl. Phys.* **91** 10157
[19] Yoneda Y, Sakaue K and Terauchi H 2003 RHEED observation of $BaTiO_3$ thin films grown by MBE *Surf. Sci.* **529** 283
[20] Lee G H, Shin B C and Kim I S 2001 Critical thickness of $BaTiO_3$ film on $SrTiO_3$(001) evaluated by reflection high-energy electron diffraction *Mater. Lett.* **50** 134
[21] Lee S-T, Fujimura N and Ito T 1995 Epitaxial growth of $BaTiO_3$ thin films and their internal stresses *Japan. J. Appl. Phys.* **34** 5168
[22] Lin W J, Tseng T-Y, Lu H B, Tu S L, Yang S J and Lin I N 1995 Growth and ferroelectricity of epitaxial-like $BaTiO_3$ films on single-crystal MgO, $SrTiO_3$, and silicon substrates synthesized by pulsed laser deposition *J. Appl. Phys.* **77** 6466
[23] Oh J-M and Nam S-M 2009 Role of surface hardness of substrates in growing $BaTiO_3$ thin films by Aerosol deposition method *Japan. J. Appl. Phys.* **48** 09KA07
[24] Huang G and Berger S 2003 Combined effect of thickness and stress on ferroelectric behavior of thin $BaTiO_3$ films *J. Appl. Phys.* **93** 2855
[25] Niu F and Wessels B W 2007 Epitaxial growth and strain relaxation of $BaTiO_3$ thin films on $SrTiO_3$ buffered (001) Si by molecular beam epitaxy *J. Vac. Sci. Technol.* B **25** 1053
[26] Vaithyanathan V *et al* 2006 *c*-axis oriented epitaxial $BaTiO_3$ films on (001) Si *J. Appl. Phys.* **100** 024108

[27] Shin W-C, Liang Y-S and Wu M-S 2008 Preparation of $BaTiO_3$ films on Si substrate with MgO buffer layer by RF magnetron sputtering *Japan. J. Appl. Phys.* **47** 7475

[28] Kim Y S *et al* 2005 Critical thickness of ultrathin ferroelectric $BaTiO_3$ films *Appl. Phys. Lett.* **86** 102907

[29] Gruverman A and Kholkin A 2006 Nanoscale ferroelectrics: processing, characterization and future trends *Rep. Prog. Phys.* **69** 2443

[30] Garcia V, Fusil S, Bouzehouane K, Enouz-Vedrenne S, Mathur N D, Barthelemy A and Bibes M 2009 Giant tunnel electroresistance for non-destructive readout of ferroelectric states *Nature* **460** 81

[31] Gruverman A *et al* 2009 Tunneling electroresistance effect in ferroelectric tunnel junctions at the nanoscale *Nano Lett.* **9** 3539

[32] Rodriguez B J, Callahan C, Kalinin S V and Proksch R 2007 Dual-frequency resonance-tracking atomic force microscopy *Nanotechnology* **18** 475504

[33] Hudson L T, Kurtz R L, Robey S W, Temple D and Stockbauer R L 1993 Surface core-level shifts of barium observed in photoemission of vacuum-fractured $BaTiO_3$(100) *Phys. Rev.* B **47** 10832

[34] Hudson L T, Kurtz R L, Robey S W, Temple D and Stockbauer R L 1993 Photoelectron spectroscopic study of the valence and core-level electronic structure of $BaTiO_3$ *Phys. Rev.* B **47** 1174

[35] Cai M, Zhang Y, Yin Z and Zhang M 2005 First-principles study of structural and electronic properties of $BaTiO_3$(001) oxygen-vacancy surfaces *Phys. Rev.* B **72** 075406

[36] Courths R 1980 Ultraviolet photoelectron spectroscopy (UPS) and LEED studies of $BaTiO_3$(001) and $SrTiO_3$(100) surfaces *Phys. Status Solidi* B **100** 135

[37] Ertl G and Küppers J 1985 *Low Energy Electrons and Surface Chemistry* (New York: VCH-Weinheim) pp 39–40

[38] Mróz S 1994 Physical foundation of quantitative Auger analysis *Prog. Surf. Sci.* **46** 377

[39] Gruverman A, Auciello O and Tokumoto H 1998 Imaging and control of domain structures in ferroelectric thin films via scanning force microscopy *Ann. Rev. Mater. Sci.* **28** 101–24